MSc FT Electronic Engineering, PSCMV Computer Vision , 2017/18

A study of increased fidelity Fourier OCT processing methods for visual discernment of white spot lesions

Research and implementation of a high resolution OCT dental imaging system

Houssem El Fekih, ID 171031393

Supervisor: Prof. Robert Donnan & Dr. Peter Tomlins

A thesis presented for the degree of
Master of Science in *computer vision*

School of Electronic Engineering and Computer Science

Queen Mary University of London

PMSF-QMELEC1 - MSc FT Electronic Engineering

Declaration of original work

This declaration is made on August 22, 2018.

Student's Declaration: I Student Name hereby declare that the work in this thesis is my original work. I have not copied from any other students' work, work of mine submitted elsewhere, or from any other sources except where due reference or acknowledgement is made explicitly in the text, nor has any part been written for me by another person.

Referenced text has been flagged by:

1. Using italic fonts, **and**
2. using quotation marks "...", **and**
3. explicitly mentioning the source in the text.

Acknowledgements

I would like to express my deep gratitude to Dr Peter Tomlins and Dr Robert Donan for allowing this unique and challenging research project and in particular Dr Peter Tomlins for providing me with enthusiastic encouragements, guidance and access to all the needed resources from the optical laboratory. Finally, I wish to thank my parents for their support and encouragement throughout my study.

Abstract

In this paper we analyse various computer vision and signal processing methods for OCT and implement improvements designed to increase the quality of the output of an optical coherence tomography system. The desired contrast and fidelity should be accurate enough to allow for reliable imaging of white spot lesions in teeth.

First the sum of all the previous work for the OCT post-processing is synthesised in a re-implementation of the current reconstruction algorithm, this allowed to delve into and explore the physical assumptions and abstractions of the interferometry process. By nature the task of ranging the interfaces is based on Fourier domain mathematics and the system transfer and be defined in terms of the convolutions, the power spectrum and its inverse and the harmonic backscatters.

An understanding the physical principles behind the image formation process is a way of finding refinements. The thesis concerns all digital post processing which works on the spectrometer readings , hence is a Digital signal processing and image processing approach to improve the quality of the signal.TODO: fixup without changing any physical setup

The main processing contribution is an implementation of a spectral reshaping interpolation method which seems to show promising CNR improvement in the wild today as for contrast enhancement and a method to compute the contrast to noise ratio to evaluate performance. In order to further improve the SNR a reflectivity a simple map correction method to correct sensitivity fall off is implemented. Finally a comparison of state of the art speckle removal methods are evaluated and implemented.

Contents

Chapter 1

Introduction

This project is building upon the work of Dr. Peter Tomlins and Dr. Robert Donnan on an implementation of Frequency based optical OCT for the purpose of detecting white spot lesion in teeth.
Most of the previous projects focused on the physical realisation of the optical tomography set-up, for example in [12] with a focus on form factor for the set-up.
Another project was focused on accelerating part of the processing using GPUs [7]. This project focused on signal-processing and computer vision methods to enhance the quality of OCT scans, without any alterations made to the optics of the system.
Optical Coherence Tomography is a recent development in non-invasive imaging that is analogous and inspired from ultrasound tomography imaging.

1.1 Motivation for this work

The current implementation of the OCT back-end incorporates a level signal correction methods and a simple reconstruction method for the 3d volume reconstruction.

1.2 Contents of the thesis

The focus of our project is on improving the algorithms used in the interferometry reconstruction process, we explores signal contrast improvement methods. We opted for implementing a recent spectral reshaping method introduced by [5]. The second part of the project we implement further image processing techniques to increase the quality, de-noise and to reach the level of discernment of white spot lesions. The first steps for this project was to learn the current reconstruction method of Optical coherence tomography, a faithful reconstruction of the current output was implemented as a learning step and as a baseline for performance. To improve the quality of the construction DSP methods were employed and to evaluate the improvement achieved, our own procedure for computing contrast to noise ratio was implemented.

Queen Mary University of London
12th August 2019

Chapter 2

Background

This thesis constrains the space of research to post processing methods that , there is ample literature [TODOATEND: citelast] on various post-processing techniques for SD-OCT which are based Digital signal and image processing techniques. While all the correction methods are Digital signal processing methods, it is still necessary to grasp a rudimentary understanding of the physical process behind OCT, more detailed explanations can be sought about the theory of OCT in [1] and [4] and the current physical realisation in [2].

2.1 OCT physical principles

OCT is a recent development in non-invasive imaging that is analogous and inspired from ultrasound tomography imaging. Since it is a light based method, it is not possible to design imaging based on the backscatter of a pulse train, because of difficulties with generation and gating the pulse train at the speed of light it is practically infeasable. The main optical OCT systems designed are based on interferometry (Michaelson's interferometer) using a steady beam with a broad bandwidth, the backscattered waves interfere constructively or destructively with the reference beam in the beam

re-combiner. back-scattering is different from normal mirror reflection in that it is in all directions including the opposite direction to the signal. OCT systems in the wild are currently of these types:

- TOCT time domain based OCT.
- SOCT spectrometer based frequency domain OCT.
- SSOCT Swept imaging based frequency domain OCT.

It is important to understand the image formation process, the following details our current understanding of how Time OCT and Spectrometer OCT work since they are of theoretical and practical interest to our set-up , details about swept imaging OCT are skipped but are available in in [1] [4].

2.1.1 TOCT

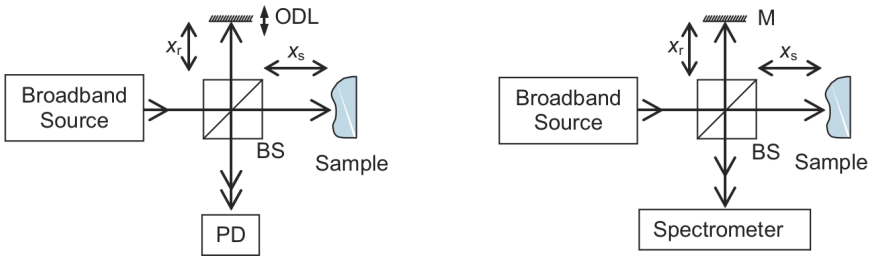

Figure 1. Representations of (A) time domain and (B) spectrometer-based spectral domain optical coherence tomography (SDOCT) systems. M, mirror; ODL, optical delay line; PD, photodetector; BS, beamsplitter.

Figure 2.1: Time OCT vs spectrometer OCT interferometer configuration

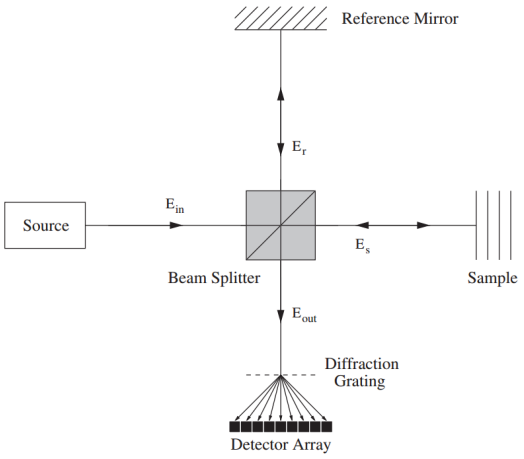

Figure 2.2: diffraction grating based spectrometer in SOCT scheme

The traditional approach is the time domain based OCT, whose operating principle is based on a beam splitter and re-combiner with variable mirror reference 2.1 to scan a particular interface at depth xdepth. the back-end re-combiner is pointed at a simple photo-diode and this has to acquire a linear 1D profile called the A-scans, one pixel at a time.
The following equation summarizes the power detected for each wave-number, Power of reference and signal are added along with an interference or coherence term.
It is a common convention in OCT literature to work in the spatial domain the source wave is modelled to be a stationary wave with zero phase velocity, the constant propagation is k is also called the wave-number k which relates to wavelength by 2π/wavelength.

this means that this wave k periods per spatial radian unit.

the spectrometer bins rather than wavelength or harmonic number, this called the wave-number k which relates to wavelength by 2π/wavelength. this means that this wave k periods per spatial radian unit.

$$P(k) = P_{ref}(k) + P_sig(k) + 2\sqrt{(P_{ref}(k) * P_{sig}(k))} * cos(k * 2 * (x_{sample} - x_{ref})) \tag{2.1}$$

where k is the wave-number, $P_{ref}(k)$ and $P_{sig}(k)$ are the wave-number power for reference and signal respectively, x_{ref} and x_{sample} are reference mirror distance and probed sample distance.

Although the expression in wave-number does not correspond to the power level detected at the photo-diode it will be useful for comprehension of SD-OCT, the power detected corresponds to the integral of the power received over the wave-numbers:

$$\begin{aligned} &P = P_{ref} + P_{sig} + 2\sqrt{P_{ref} * P_{sig}} * \\ &sinc(\pi(X_{ref} - x_{sample}/l_c) * cos(k_0 * 2(x_{ref} - x_{sample})) \end{aligned} \tag{2.2}$$

where k_0 is the mean wave-number and l_c is the coherence length which is equal to $\pi/\delta k$ (the bandwidth). The key variable for resolution of the system is the coherence length l_c which is why a wide bandwidth for the source light is selected.

We can see that in an TD-OCT scheme inference has to happen at one sampling interface at a time collecting simultaneously the power and location of samples by finding the envelope of the peaks. But this means that for a scan line the system has to spend probing each interface depth by moving the mirror.

2.1.2 SOCT

In the implemented scheme by the current implementation the SD-OCT uses a diode generated beam with a wide bandwidth central wavelength of $1325nm$ over a bandwidth $> 100nm$. In the SD-OCT scheme it which the main reason for its popularity. As you can see in 2.1 and 2.2 instead of a movable mirror and a photo-diode the system uses a fixed mirror and a spectrometer (made

from a diffraction grating and CCD array). The Spectrometer records the spectral variation of the signal as shown in equation 1. The period of the spectral variation is proportional to $x_{sample} - x_{ref}$ therefore an FFT of the spectral variation will produce a scan-line equivalent to TD-OCT output.

The above derived equation is based on the measure of irradiance of the electric field through the optical system and backscattered, at the detector the power is the sum of the reference mirror reflection and source power as well as the autocorrelation function of the electric field at the Electric field at the time delay between reference mirror and scanning interface. denoted: $\gamma_{11} = (E_r(t), E_s(t+\tau)$ where τ represents the time delay between the interferometer arms (sample and reflection).

This measure of autocorrelation, corresponding to the interferometric and coherence term in the above equation, for a stationary random signal, through the Weiner-Krichn theorem establishes the following equivalence: $\int_{\infty}^{inf} P(k) * e^{-kx} \mathrm{d}k \leftrightarrow DC + \gamma_{11}(x) = \int P(w) x e^{-iwx/c} \mathrm{d}w$

The above equation's Fourier transform can be view as the integral of the signal at each wave-number which is γ_{11} . Through the Weiner Kirch theorem this autocorrelation function is equivalent to the power spectrum times the interference term $cos(2xkx(x_s - x_r))$ the mathematical derivation is explained for the principles behind OCT are explained from the ground up from monochromatic light, adding multiple frequency modulation and full-bandwidth OCT system in chapter 3 and 4 of [4] In summary, the received signal's transfer function is the Fourier transform of above equation, it can be viewed a windowing of the interference components reflected from the sample and the source power spectrum.

This view is central to the spectral reshaping method explained in section 3.1 more formally [5] defines the accumulated interference terms as $d(k) = p/2 \sum \sqrt{R_r * R_{sj}} x(cos(2xk(z_r - z_{sj})))$ the IOCT system find the depth scan profile as the Fourier transform of the detected signal $I_{oct}(z) = FFT[i_{oct}(k)] = S(z) * D(z)$, $D(z) = \sum p/4 \sqrt{(Rr * Rs)} \delta(z + -2(zr - zsj))$

a digital signal processing perspective as the the convolution of the inverse Fourier transform of the power spectrum or and backscattered harmonic signals from sample. For simplification and by duality the inverse Fourier transform and forward FT operation is used in many OCT papers.

A re-sample from wavelength to k space has to occur because of the non linear diffraction of the grating. A correction is done through a re-sampling table computed on an equal bandwidth signal with no interference before an FFT is computed, of which the envelope gives an A-scan equivalent to TOCT output. Details of the re-sampling table computation are available in [7] and 2.3.1 The interference working describe how a linear 1-D slice of resolution equal to CCD length (1024 in our set-up) in TOCT or SOCT. These images are then put together into one B-scan as can be seen in 2.3. As you can see this provides a series of line slices each 1024 long, the top pixels representing the closest x_{sample} interface probed.

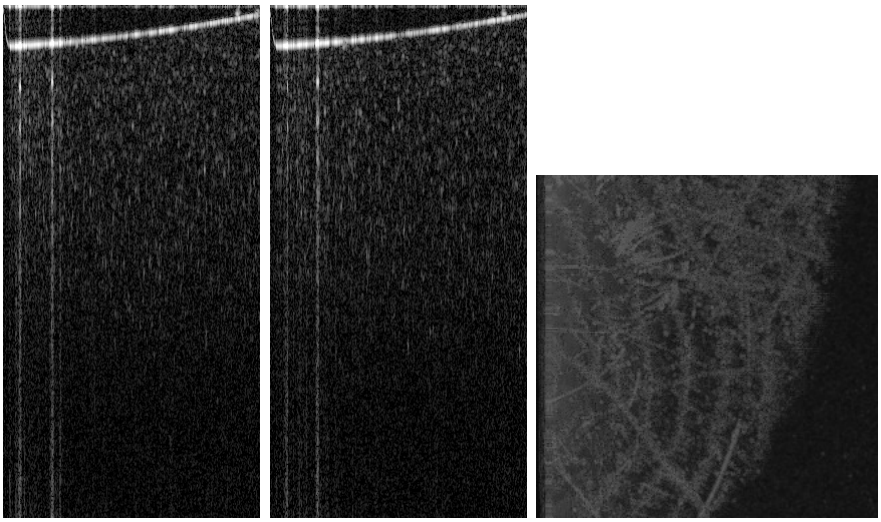

Figure 2.3: two left images represent a B-scan , a contiguous series of A-scans acquired by the probe showing a side view of top-down acquisition of a random phantom disk, to the right is a sum image of all the A-scans from the top

2.2 Windowing

The SD-OCT computational reconstruction involves an inverse Fourier transform of the output of the spectrometer, the spectrometer is a diffraction grating pointed at a 1D CMOS array of 1024 pixels. As described in section after re-sampling the data with a reference spectrum in 2.3.1 The discrete Fourier transform assumes a periodic wave, and in the case of an aperiodic signal a DFT is an equivalence relation to an assumed infinite signal of the repeat aperiod signal, making a periodic transform pair. Furthermore a Discrete Fourier transform is a sampling of filter banks bins of $\delta f = 1/T_{span} = n\delta t$ where n is the number of samples and δt the constant time between samples. If the signal was periodic, it would have an exact number of harmonics and the sampling does not cause any spectral smearing, which does not occur except for a periodic signal Fourier series.

The truncation of the signal at the ends creates a sharp boundary and introduces high frequency noise into the DFT output, and the discreteisation of the bins is the equivalent of a multiplication with a rectangular window for each of the bins whose frequency response has a high side lobe amplitude, this means that each bin of the filter bank, is convolved with such responses, this aliased information into the bin from side bin. The frequency response of the rectangular window can be seen in 2.4 and demonstrates the problem addressed by windowing.

The solution in digital signal processing is to convolve the signal with a window function, a window function is chosen based on its frequency response balancing between spectral resolution , width of the main lobe and spectral leakage.

2.5 shows an example of the effect of applying a hamming window on the acquisition of data, this window is not to be confused with Hanning window.

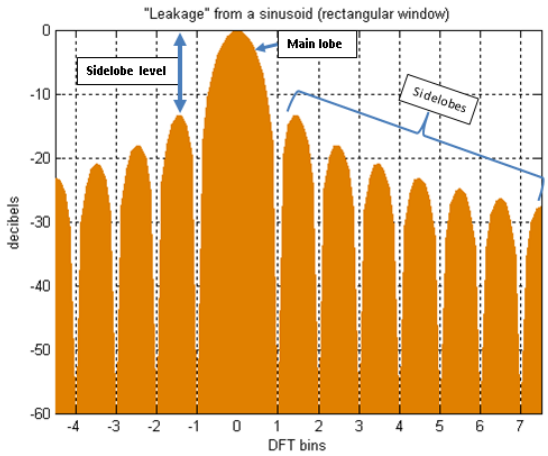

Figure 2.4: demonstration of main and side lobes in the Fourier pair of the rectangular window function

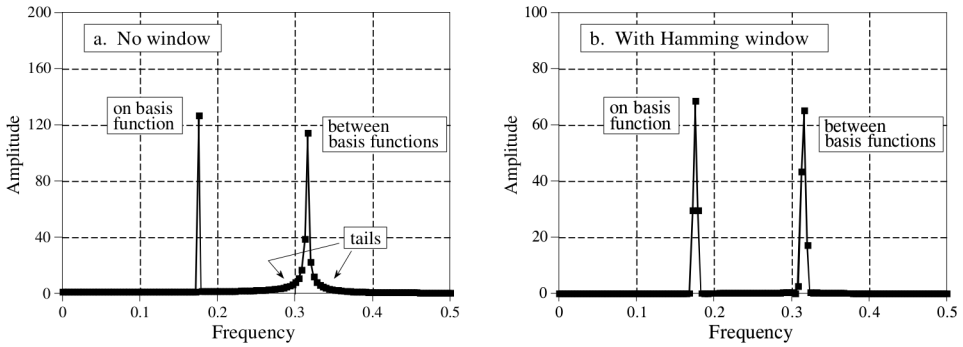

FIGURE 9-4
Example of using a window in spectral analysis. Figure (a) shows the frequency spectrum (magnitude only) of a signal consisting of two sine waves. One sine wave has a frequency exactly equal to a basis function, allowing it to be represented by a single sample. The other sine wave has a frequency *between* two of the basis functions, resulting in *tails* on the peak. Figure (b) shows the frequency spectrum of the same signal, but with a Hamming window applied before taking the DFT. The window makes the peaks look the same and reduces the tails, but broadens the peaks.

Figure 2.5:

2.3 Current signal processing

To build on the existing work in the signal processing of the system it was first needed to comprehend and to port existing back-end. The existing back-end was scattered across many iterations with many differing implementations done by different people for different purposes, some implemented on GPU and others in matlab, the version that is live in the lab is a sped-up C sharp GPU implementation. It contained all of the straightforward correction techniques and it was very useful to reimplement them in python in order to grasp the digital processing tasks involved the following section presents the computational steps involved based on a simplified matlab script version.

2.3.1 Functional flow

Re-sampling

Due to the physical set-up of the diffraction grating , the spectrum recorded in the spectrometer is un-even in k-space. Therefore a re-sampling operation is precomputed on the spectrum where the source spectrum is recorded with a mirror. This operation records the spectrogram of the source and pre-computes a re-sampling table which is even. This re-sampling table associates a real spectrum location value to a bin. This is such that the real captured signal is cubically interpolated at those offsets in order to render an evenly spaced Fourier domain bin for the inverse transform. This is essentially a tuning step that corrects the imperfection caused by the nature of the diffraction grating spectrometer and the output captures the real Fourier domain spectrum of the signal captured.

Deconvolution

The next step that you can see in code below is to deconvolve with the reference spectrum, as explained in the SDOCT introduction the output is

equivalent to the convolution of the source bandwidth inverse transform and the harmonics interference of backscattered signal. This step is computing the deconvolution operation by dividing the capture output with the reference spectrum obtained through the mirror calibration operation. Since the operation is in the Fourier domain, it is a point-wise multiplication of the output with the reference spectrum.

Windowing

The next part as explained in 2.2 is to window the signal. In the previous iteration of the software the window function chosen was tunable from the GUI and was by default a nuttall window. This window has the shape and Fourier characteristics shown in 2.6

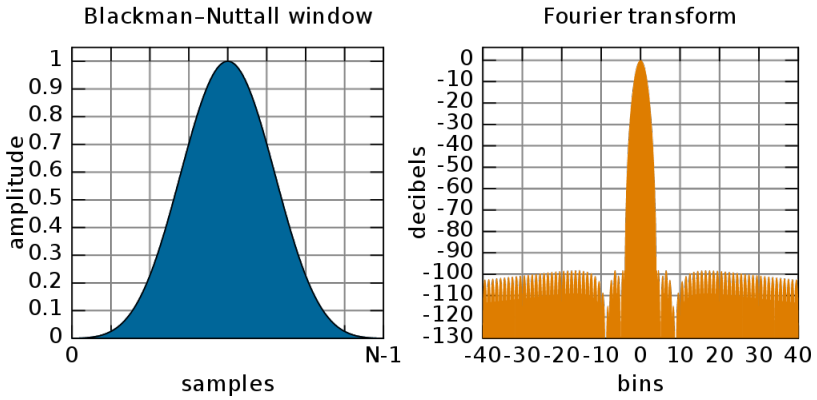

Figure 2.6: Nuttall window and Fourier response

A figure will be included showing the drastic effect of not having windowing.

Signal extraction

As explained in the depth profile A-scan can be obtained by a Fourier transform of the signal, the envelope of the complex output spectrum is the depth

profile it is however very faint and not representative in the visual domain. In order to compress the signal and represent the grayscale levels in a meaningful manner it is necessary to compute the power spectrum in decibel 20 * log (envelope) And to stretch it to fit a reasonable range of decibel, this is still an area of research in signal extraction and we hope to fully clarify for final report.

```
function
    [linAScanEnvelope,logAScanEnvelope,ascan]=ProcessOCTAScan(spectrum,resamplingTable,r
    window)

        spectrumLength=max(size(spectrum));
        ascanLength=floor(spectrumLength/2);

        % Deconvolve
        deconv=(corrected ./ referenceSpectrum);

        meanDeconv=mean(deconv);
        %
        % Mean centre
        %
        meanCentred=deconv-meanDeconv;

        % Resample
        resampled=spline(resamplingTable(:,1),meanCentred,resamplingTable(:,2));

        % Window
        windowed=resampled .* window; % this is a nuttall window in
            the released software
```

```
        % Fourier transform
        ft=fft(windowed);

        ascan=ft(1:ascanLength);

        logAScanEnvelope=20*log10(linAScanEnvelope);

end
```

2.3.2 Our port

For comparison you can below snippets of the code that relates to the A-scan reconstruction Our implementation for the processing defined a base class *basic_correct.py* in the *src.basic_correct.py* package and it is general enough to provide implementation inheritance to the paper implementation of spectral correction method shown below 2.3.2

```
lass AScan:
  def __init__(self,ref_spectrum,resample,imrange):
    self.ref_spectrum = ref_spectrum
    self.resampling_table = resample
    self.range = imrange

  def deconv_threshold(self,spectrum_val,ref_val):

    if ref_val> 0.1:
      return float(((spectrum_val + 1000.0) / (ref_val + 1000.0)) -
          1.0)
    else:
      return 0.0

  def deconv_method(self,spectrum):
```

```
    # method by which the source spectrum is deconvolved from IOCT
        signal
    deconv = [
        self.deconv_threshold(spectrum[i],self.ref_spectrum[i]) for
        i in range(len(spectrum))]

    deconv = deconv - np.mean(deconv)

    nuttall = signal.nuttall(1024)
    windowed = [ (deconv[i] * nuttall[i]) for i in
        range(len(spectrum)) ]

    np_deconv = np.array(windowed,dtype='float32')


    return np_deconv

  def a_scan(self, spectrum):
    np_deconv = self.deconv_method(spectrum)

    spline = interpolate.splrep(np.arange(0,1024), np_deconv, s=0)
    xnew = np.array(self.resampling_table, dtype='float32')
    self.deconv_interpolated_spectrum =
        np.float32(interpolate.splev(xnew,spline))
    return self.correction_method()


  def fftenvelope(self,spectrum):
    positive_complex_freqs = fftpack.fft(spectrum)[0:512]
    return np.abs(positive_complex_freqs)

  def clip(self,val):
```

```
    if val > 255:
      return 255
    if val <= 0:
      return 0
    else: return int(val)

  def grayscale_range_stretch(self,nparr):
    minv = self.range['min']
    maxv = self.range['max']

    minv = -60
    maxv = -10
    span = 40
    return np.array([self.clip(grayscale) for grayscale in
        ((span/255) * (nparr - minv))], dtype='float32')

  def to_grayscale(self,signal):
    powervals = 10 * np.log10(signal * signal , dtype='float32')
    out = self.grayscale_range_stretch(powervals)

    return out

  def correction_method(self):
    signal = self.fftenvelope(self.deconv_interpolated_spectrum)
    return self.to_grayscale(signal).astype("int")
```

Optical characteristics of the system

The system transfer function or impulse response is the output of the imaging system in the presence of a single impulse, typically The two-dimensional delta function is an image composed of all zeros, except for a single pixel at: row = 0, column = 0, which has a value of one. The point spread function

is the optical jargon of the natural 2d extension of the idea of a impulse response, the resulting image in the system is the result of the shifted impulse response weighted by the impulse light intensity at each pixel. When a point is convolved with the PSF, it spreads out, this is why the impulse response is often called the point spread function (PSF) in image processing jargon. In order to characterise the signal a PSF function was computed in [2] a PSF is characterised by its Full width at half maximum denoted FWHM. A B-Scan is ranging a space of width of 3 mm acquired over 500 A-scans, yielding a nominal lateral pixel size of 6.9 m. For comparison, the axial pixel size is 9.5 m.

The overall system PSF has been measured to have a FWMH of 7.8 µm + 1 axially and 9.1 µm + 1.7 laterally Displacement precision was greater laterally compared to axially. This is because the lateral pixel spacing (6.9 µm was 24% smaller compared to 9.1 µm than the lateral PSF FWHM (9.1 µm), as for the axial pixel spacing it is 21% larger than the axial width of PSF of 7.8 µm. than the corresponding axial PSF FWHM (7.8 m). Thus, laterally, the PSF FWHM is sampled more than once due to the pixel spacing, but axially the PSF FWHM is under-sampled.

The lateral over sampling will result in cross talk between adjacent spectrometer tracks and is among the reasons for imprecisions in the system.

2.4 K-means clustering algorithm

An explanation of the EM K-means unsupervised clustering algorithm will be provided.' There was an attempt to incorporate spatial features to the clusters and not just histogram value clustering but this is hard to fine tune to specific image. There is also the possibility of using the otsu thresholding method based on fischer criteria, this comparison will be supplied.

2.5 Contrast to noise ratio

In order to measure the quality of the B-Scan image grab, one indicative metric is the contrast to noise ratio, it is defined as the contrast between the mean value in foreground object region and background object region divided by the noise. The images whose quality we seek to improve are of teeth, and it is fortunate that teeth at the imaging depth we seek presents two main regions of contrast, the top layer of enamel and the dentine, this is simplified ignoring other artefacts. In order to provide a correct segmentation of the images a Kmeans clustering algorithm was used, and it yields segmentation similar to this

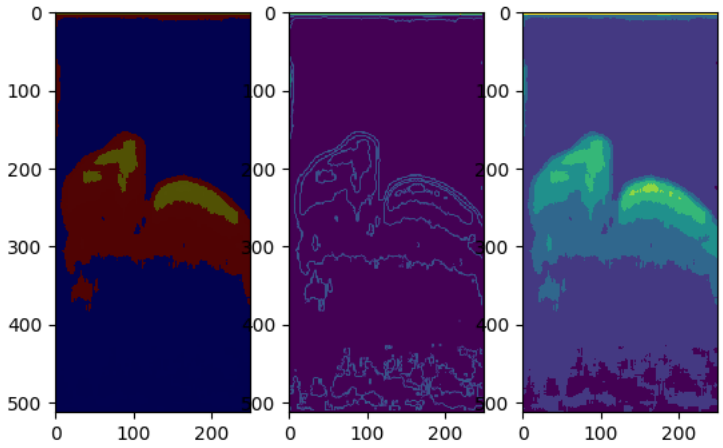

Figure 2.7: An example of tooth segmentation, on the left the three cluster pixel segments can be discerned, in the middle the sobel edge map and a gaussian blurred of the image to visually highlight possible regions.

This method shows good segmentation, but it has two issues, one is the potential to discern between background object and noise, and the other is the random aspect of K-means, and in order to provide a consistent metric we opt for fixing the random seed to be the min max and median value of the

image. This guarantees a deterministic segmentation for any given image. which makes the metric useful for comparing effectiveness of correction. In order to test the implementation of CNR code we ensured that the CNR of an image and of its blurred equivalent was inferior.

Chapter 3

Image quality improvement methods

There are many sources of inaccuracies in the IOCT system. the main physical ones which are not addressed beyond resampling are :

polarisation

dispersion

Grating and other optics artefacts

CMOS noise/quantisation

multiple scattering

motion artefacts

The main computational ones for a single A Scan:

inaccuracies due to source coherence length

windowing

ADC conversion

DC noise

depth sensitivity fall-off

For a B-scan this is compounded by lateral resolution oversampling, and doppler effects that can be significant in the acquisition time.

3.1 Advanced signal reshaping method implementation

3.1.1 Overview

Our main contribution to this date is the implementation of a spectral reshaping method based on [5]. This method works by building on existing spectral reshaping methods. Spectral shaping signal processing technique yields a higher contrast OCT signal, As explained in section 2.1.2 the interferometry process can be seen as a multiplication of the power spectrum and the backscatter signal at each wave-number, this is the equivalent of a windowing of the backscatter harmonic signal with the power spectrum of the source. In the Fourier domain the envelope signal is convolved with the power spectrum. Spectral reshaping is typically done with a Gaussian window, because a gaussian window has desirable smoothing properties, namely that it's Fourier transform is gaussian. it computes a window that is the ratio between the reference spectrum and an ideal Gaussian spectrum. This means that windowing with this window reshapes the source spectrum contribution to a Gaussian that is fitting the reference spectrum (first and second moment mean and variance). This method refines the spectral reshaping method defined in [9]. It reshapes the source spectrum to an ideal hanning window which presents good tradeoff between contrast (main lobe width) and spectral resolution. a hanning window has the following profile 3.1

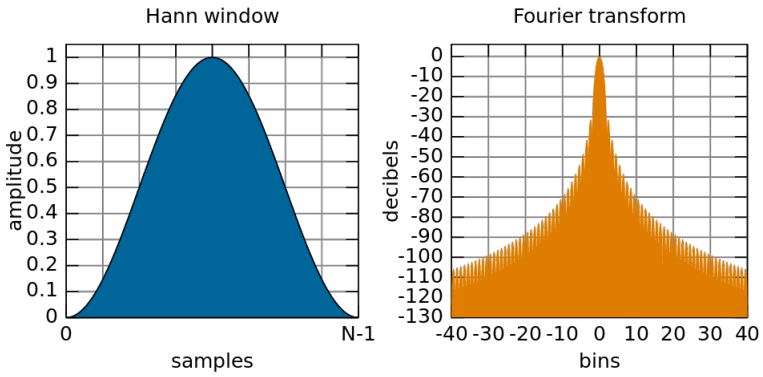

Figure 3.1: Hanning window and Fourier response

This is however only the initial phase of the correction method. since a hanning window was chosen to be the ideal spectrum which is convolved with the harmonic backscatter, It was already demonstrated that the output of the FFT of the signal was a windowing of the harmonics of the backscatters with the power spectrum. The previous steps have reshape the power spectrum to be an ideal hanning window. The nice property of the hanning window is computing the barycenter of two points in the main lobe returns 0, the real maximum peak of the signal, this allows to recover the real peaks This in turn allows the synthesis of an further interpolation of the real amplitude of the peaks. The interpolation is a barycentric interpolation of adjacent points to peaks that locates the real peak location. This real peak is evaluated using the known real value of the peak at the interpolated location. This yields a higher CNR value and good axial resolution. One challenge found is to ensure to pick the real peaks and not noise peaks which problematically lie in the very low values which at the limit of the function in zero tends to infinity. a basic thresholding method is used to find real peaks instead of noise and this yields results like the following:

TODO: put figure here

3.2 ADC

3.2.1 Power values

The output of the interferometer ranging data is very faint since it represents intensity values of the electric field at different ranges. Therefore it is necessary to translate the values in a dynamic range that is suitable for visual representation in grayscale. The common method employed in digitisers** is to calculate the logarithmic power of data and to then use contrast range stretching or histogram equalisation to map the decibel values into the valid grayscale range (0-255). The formula for the logarithmic power operator is the following: $(20 * log10(power * power))$**

3.2.2 Range mapping

The purpose of range mapping is to map the decibel values of the Fourier reconstruction power value output to [0,255] (or for any bit-precision 2^L to [0 ,L-1]).

ADCclasses are found in package 'src.ADC', three methods are provided and compared for efficiency, the methods operate on a full B-Scan allowing potential B-Scan wide range adjustment. all the ADC classes provide a 'to_img' method which implements the stretching:

Contrast range stretching - ported method

Contrast range stretching can be implemented in two ways, the first way used in the original codebase and that is ported in the ADC class *contrast_stretch_ADC.py* this method works by assuming a minimum threshold level, which is fixed to -90db. It also assumes that the dynamic range is fixed to 100. The resulting output values are computed as follows: $stretched = span/255 * (b\_scan\_power - minv)$ where minv = 90 and span = 100.

the output of this mapping can be below 0 for any decibel value ¡ -90db

and bigger than 255 for any value outside the span range, which are the pixels that are bigger than -90db + 100db = 10db.

Those values that lie outside the range are clipped, which means that the range mapping acts as a filter for low amplitude noise and high values.

This method produces good results despite being arbitrary in the range of values it considers and is not sensible to outlier values.

Contrast range stretching - full-range method

The second method for contrast range stretching works by mapping the lowest value in B-Scan to 0 and the highest to 255, This provides the maximal amount of dynamic range by using the full range. However it could be sensible to outlier values (eg DC, in unfiltered DC signal). notice the ratio of span to values is flipped, and the minimum and span values are calculated to be the B-Scan wide minimum and range:

```
minv = np.min(np_b_scan)
span = np.max(np_b_scan) - minv
stretched = (255 / span * (np_b_scan - minv)).astype('int')$
```

The disadvantage of this method in the presence of outliers, it will stretch the values and result in low intensity of pixels for high pixels and the opposite for low pixels. The way to mitigate this effect is to choose the span and minimum such as outliers are discarded, this is done by considering the range of 5% for minimum and 95% for maximum percentile, which means some values of the data pixels need to be clipped as well.

3.3 Depth sensitivity fall-off

The optics of the spectrometer, the diffraction limit and the size of the pixels impose constraints on the depth of imaging that is realisable, this is due to imperfections in collimating lens which impose a stochastic process on

wave diffraction and the discretisation is imposing a rectangular sampling of incident photons. This is explained in more details in Kenny, [**?**]. As a summary of both the Gaussian distribution of the incident light shape and the rectangular windowing of the beam at each pixel is analytically summed to be an attenuation of sensitivity as a function of depth: $R_{spectrometer} = \sin \delta x P z / \sin \delta x P z \exp -a^2 P^2 z^2 / 4 \ln 2$

A depth map of a mirror are collected, they indicate a fall off in backscattered signal power dependent on depth, A maximum map of mirror reflections has been compiled from multiple grabs of a reflector at , The fall off can qualitatively be assessed to be pronounced.

3.4 Speckle noise removal

Once the Fourier interferometry and ADC conversion have acquired an image, it can be observed that speckle artefacts are pronounced in the image, the speckle while pronounced is not immediately clear what type of noise it is. From the physical standpoint, speckle are the result of multiple scattering objects being close to the coherence length and there are ways to change the As explained in [10] it is possible to change the physical setup to obtain a more precise noise distribution from a compound incoherent sources assuming a Rayleigh distribution of the scattering.

This type of methodology is not sought as it involves and we constrained our analysis to

Chapter 4

Potential improvements

4.1 physical methods of improvement

4.1.1 wave-number re-sampling

Since the spectrometer in SOCT methods is usually built from a diffraction grating and a collimating lens, the incident beam's separation in wavelength is non-linear, As explained in the re-sampling section 2.3.1 we used the previous work of interpolating the appropriate wave-number locations of the beam explained in [7]. A physical solution to the problem would be to build a linear in wave-number spectrometer, as was done by [11]. This approach works by adding a prism to the spectrometer which inverses the known dispersion relationship of the angle of light is non linear in number of grooves and incident angle. This non-linearity means that the resulting bandwidth is uneven, but it is infeasable to design spectrometer with variable pixel size. By adding an appropriately designed prism a linear in wave-number spectrometer is made. This allows to improve the fall-off moving the -6db sensitivity fall off from 1.35 mm to 1.7mm as can be seen in 4.1.1.

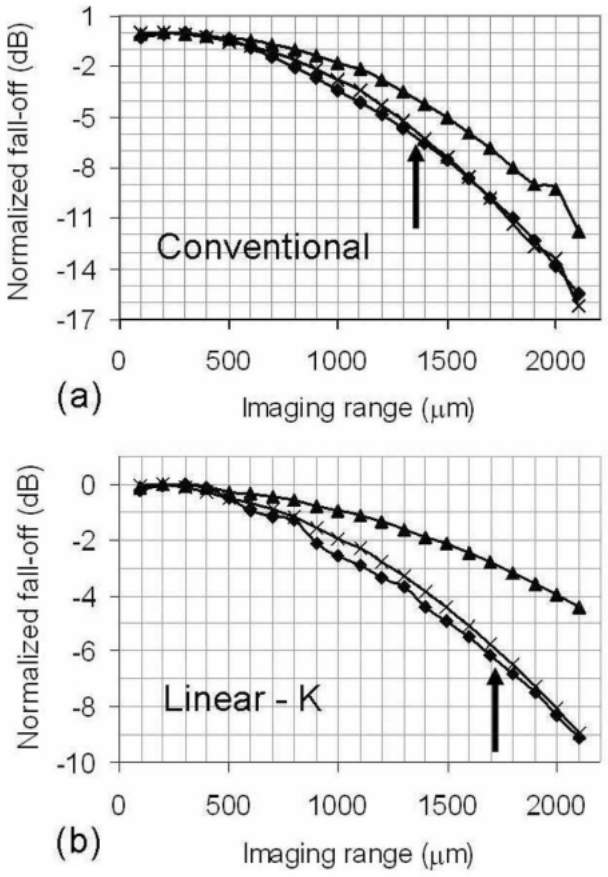

Fig. 3. Falloff simulations and experiments for (a) conventional and (b) linear-k spectrometers at spectrometer optical resolutions of 12.5 μm (triangle) and 35 μm (cross and diamond). Experimentally measured falloff marked by diamonds. Arrows mark experimentally determined –6 dB falloff ranges.

Chapter 5

Conclusions

Vivamus vehicula leo a justo. Quisque nec augue. Morbi mauris wisi, aliquet vitae, dignissim eget, sollicitudin molestie, ligula. In dictum enim sit amet risus. Curabitur vitae velit eu diam rhoncus hendrerit. Vivamus ut elit. Praesent mattis ipsum quis turpis. Curabitur rhoncus neque eu dui. Etiam vitae magna. Nam ullamcorper. Praesent interdum bibendum magna. Quisque auctor aliquam dolor. Morbi eu lorem et est porttitor fermentum. Nunc egestas arcu at tortor varius viverra. Fusce eu nulla ut nulla interdum consectetuer. Vestibulum gravida. Morbi mattis libero sed est.

Bibliography

[1] Zahid Yaqoob, Jigang Wu, and Changhuei Yang *Spectral domain optical coherence tomography: a better OCT imaging strategy*, California Institute of Technology, Pasadena CA, USA, BioTechniques 39:S6-S13 (December 2005).

[2] Peter H. Tomlins, Mohammed Wahidur Rahman and Robert S. Donnan *Dynamic measurement of local displacements within curing resin-based dental composite using optical coherence elastography*, J.Biomed. Opt. 21(4), 046001 (2016), doi: 10.1117/1.JBO.21.4.046001

[3] Pierre Wickramarachi, Data Physics Corporation, San Jose, California *Effects of Windowing on the Spectral Content of a Signal*

[4] Brezinski, Mark E *Optical Coherence Tomography : Principles and Applications, Elsevier Science and Technology, 2006*

[5] Ni, G., Liu, L., Yu, X., Ge, X., Chen, S., Liu, X., et al. *Contrast enhancement of spectral domain optical coherence tomography using spectrum correction.*, Computers in Biology and Medicine, 89, 505-511, http://hdl.handle.net/10220/44293

[6] Stephen W. Smith *The Scientist and Engineer's Guide to Digital Signal Processing* www.dspguide.com

[7] Shamitha Akalana Ranasinghege Don *Development and assessment of a Graphics Processing Unit accelerated correlation mapping Optical Coher-*

ence Tomography processing and rendering pipeline, BEng FT Electronic Engineering with Industrial Experience, Supervisors: Dr Robert Donnan & Dr P.H. Tomlins.

[8] Ruye Wang *Histogram equalisation, 2016-09-29* http://fourier.eng.hmc.edu/e161/lectures/contrast_transform/node2.html

[9] Renu Tripathi, Nader Nassif, J. Stuart Nelson , Boris Hyle Park and Johannes F. de Boer *Spectral shaping for non-Gaussian source spectra in optical coherence tomography* OPTICS LETTERS / Vol. 27, No. 6 / March 15, 2002 2002 Optical Society of America

[10] Speckle reduction in optical coherence tomography by frequency compounding Article in Journal of Biomedical Optics · August 2003 DOI: 10.1117/1.1578087 · Source: PubMed

[11] Hu, Zhilin and Rollins, Andrew, *Fourier domain optical coherence tomography with a linear-in-wavenumber spectrometer* Article in Optics Letters · January 2008 DOI: 10.1364/OL.32.003525 · Source: PubMed

[12] Robert Christopher Jones *Developing an in vivo OCT probe for imaging oral disease*